Radial basis collocation method for dynamic analysis of axially moving beams

Lihua Wang†

School of Aerospace Engineering and Applied Mechanics, Tongji University, Shanghai, China

Jiun-Shyan Chen‡

Civil & Environmental Engineering Department, University of California Los Angeles (UCLA), Los Angeles, CA 90095, USA

Hsin-Yun Hu†‡

Mathematics Department, Tunghai University, Taichung 4011, Taiwan, R.O.C.

(Received September 1, 2009, Accepted September 17, 2009)

Abstract. We introduce a radial basis collocation method to solve axially moving beam problems which involve 2nd order differentiation in time and 4th order differentiation in space. The discrete equation is constructed based on the strong form of the governing equation. The employment of multiquadrics radial basis function allows approximation of higher order derivatives in the strong form. Unlike the other approximation functions used in the meshfree methods, such as the moving least-squares approximation, 4th order derivative of multiquadrics radial basis function is straightforward. We also show that the standard weighted boundary collocation approach for imposition of boundary conditions in static problems yields significant errors in the transient problems. This inaccuracy in dynamic problems can be corrected by a statically condensed semi-discrete equation resulting from an exact imposition of boundary conditions. The effectiveness of this approach is examined in the numerical examples.

Keywords: radial basis function; collocation method; axially moving beam; strong form.

1. Introduction

Axially moving beams exist in many mechanical systems, where the vibration characteristics and dynamic stability are of critical importance to those systems. The traveling flexible string and traveling tensioned Euler-Bernoulli beam are the typical models for such axially moving continua. Ozkaya and Pakdemirli (2002) obtained an analytical form of solution using the Lie group theory. Kong and Parker (2004) introduced a perturbation method to obtain the eigensolutions of axially

---

† Graduate Student
‡ Professor, Corresponding author, E-mail: jschen@seas.ucla.edu
†‡ Assistant Professor

moving beams with small bending stiffness. Other approaches have been proposed by using the modal analysis (Wickert and Mote 1991), the assumed modes method (Gurgoze 1999, Yuh and Young 1990), the Rayleigh-Ritz method (Yoo 1995, Sylla and Asseke 2008), the modified Galerkin's method (Zhu and Ni 2000, Wang *et al*. 2009), the spectral element method (Lee and Oh 2005, Lee and Jang 2007), the finite element method (Rao 1992), and adaptive refinement technique for solving moving beam problems (Stylianou and Tabarrok 1994).

The above mentioned numerical methods are of Galerkin type weak formulation. An alternative approach which constructs discretization of PDEs directly based on the strong formulation, collectively called the collocation method, has become popular since the pioneering work of Kansa (1990) using the multiquadrics radial basis function (MQ RBF). The investigation of RBFs can be tracked back to Hardy (1971) on MQ RBF for topographical surfaces approximation based on scattered data. Following Kansa (1990), RBFs have been widely used as the basis functions for solving partial differential equations (Hon and Schaback 2001, Fasshauer 1999, Hu *et al*. 2007). The mathematical theories for convergence in the RBF approximation can be found in Madych and Nelson (1992). Raju *et al*. (2003) introduced a radial basis function meshless local Petrov-Galerkin method to solve Euler-Bernoulli beam problems and showed a great simplicity of using RBF compared to moving least-squares interpolations for approximation. Tiago and Leitao (2006) presented radial basis functions for nonlinear structural problems. Liu *et al*. (2005) introduced the radial basis collocation method for the analysis of microelectromechnical systems. A radial spline collocation method has been investigated by Wu *et al*. (2008) for the static beam analysis as an improvement of the conventional spline collocation method. Ferreira (2003) proposed a meshfree method based on radial basis function for the analysis of thick laminated composite beams under a first-order shear deformation theory. Hu *et al*. (2007) proposed a weighted radial basis collocation method to reduce errors on the boundaries of boundary value problems. Chen *et al*. (2008) introduced a localized RBF approximation which possesses polynomial reproducibility while maintaining the exponential convergence and improving the conditioning of the discrete system. This approach, combined with a subdomain collocation method, has been proposed by Chen *et al*. (2009) for solving problems with heterogeneity.

In this work, the radial basis collocation method is proposed for the dynamic analysis of axially moving Euler-Bernoulli beams. The radial basis collocation method is introduced for spatial discretization, while Newmark method is employed for temporal discretization. Since in radial collocation method the number of collocation points needs to be much larger than the number of source points for desired accuracy, the discrete system is over-determined and is solved by the least-squares method for an approximate solution. This yields errors on the boundary solution. We show that this error in the least-squares treatment of boundary conditions can propagate in space and in time. In this work, the semi-discrete equation is first statically condensed by imposing boundary conditions, and the full discrete equation is then constructed by temporal discretization and solved by a least-squares method. The numerical results show a significant improvement in this approach compared to the imposition of boundary conditions by the weighted boundary collocation method.

This paper is arranged as follows. The radial basis functions are introduced in Section 2, and their convergence in function approximation and its higher order derivatives are demonstrated. In Section 3, the general framework of radial basis collocation method for elasto-dynamics is presented, and the treatment of boundary conditions is also discussed. Several axially moving beam problems are analyzed in Section 4 to examine the effectiveness of the proposed method. The concluding remarks are given in Section 5.

2. Radial basis approximation

The radial basis function (RBFs) have been widely used for interpolating highly irregular scattered data and for solving partial differential equations. Most RBFs are infinitely continuously differentiable global radial functions, for example,

$$\text{Multiquadrics (MQ): } g_I(\mathbf{x}) = (r_I^2 + c^2)^{n-\frac{3}{2}}, \quad n = 1, 2, \cdots \tag{1}$$

$$\text{Gaussian: } g_I(\mathbf{x}) = \begin{cases} \exp\left(-\dfrac{r_I^2}{c^2}\right) \\ (r_I^2 + c^2)^{n-\frac{3}{2}} \exp\left(-\dfrac{r_I^2}{a^2}\right) \end{cases}, \quad n = 1, 2, \cdots \tag{2}$$

$$\text{Thin plate splines: } g_I(\mathbf{x}) = \begin{cases} r_I^{2n} \ln r_I \\ r_I^{2n-1} \end{cases}, \quad n = 1, 2, \cdots \tag{3}$$

$$\text{Logarithmic: } g_I(\mathbf{x}) = r_I^n ln r_I, \quad n = 1, 2, \cdots \tag{4}$$

where $r_I = \|\mathbf{x} - \mathbf{x}_I\|$, the constants c and a are called the shape parameter, and $\mathbf{x}_I$ is called the source point in the RBF literatures. The RBF approximation of a function u, denoted as u^h, is expressed as

$$u^h(\mathbf{x}) = \sum_{I=1}^{N_s} g_I(\mathbf{x}) \alpha_I \tag{5}$$

The work by Madych and Nelson (1992) shows an exponential convergence rate in RBF approximation if RBF is globally analytic or band-limited.

The application of RBF to partial differential equation is natural as the RBFs are infinitely differentiable ($g_I(\mathbf{x}) \in C^\infty$), where the derivatives of approximation are

$$\frac{d^n u^h(\mathbf{x})}{dx^n} = \sum_{I=1}^{N_s} \frac{d^n g_I(\mathbf{x})}{dx^n} a_I \tag{6}$$

Here the derivatives of RBFs can be easily calculated. The derivatives of the MQ RBF are shown in Fig. 1.

To demonstrate the convergence properties of RBF, we approximate a function

$$u(x) = \sin x, \; 0 \le x \le \pi \tag{7}$$

which describes the fundamental vibrating beam behavior. We consider the following collocation method for RBF approximation of u

$$\sum_{I=1}^{N_s} g_I(\hat{\mathbf{x}}_J) a_I = \sin(\hat{\mathbf{x}}_J), \text{ for } J = 1, \ldots, N_c \tag{8}$$

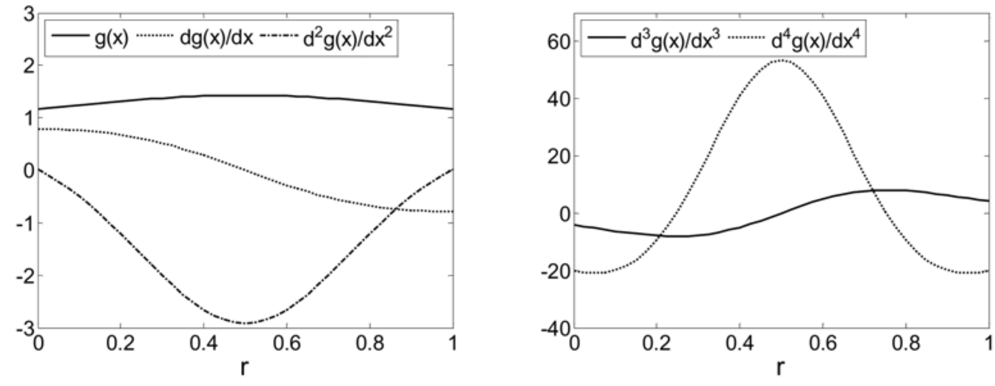

(a) (b)

Fig. 1 MQ RBF: (a) function centered at $\mathbf{x}_I = 0.5$ and its 1st and 2nd order derivatives; (b) 3rd and 4th order derivatives

where $\hat{\mathbf{x}}_J$ is called the collocation point, and N_c is the number of source points, and N_c is the number of collocation points. Eq. (8) can be expressed as

$$\mathbf{A}\mathbf{a} = \mathbf{b} \tag{9}$$

where $\mathbf{a}$ is coefficient vector to be determined , $A_{IJ} = g_J(\hat{\mathbf{x}}_I)$, $b_I = \sin(\hat{\mathbf{x}}_I)$, and $\mathbf{A}$ is with dimension $N_c \times N_s$. For sufficient accuracy, $N_c > N_s$ needs to be used, and (9) becomes an over-determined system which can be solved by, for example, least-squares method, by minimizing the following error

$$E = (\mathbf{A}\mathbf{a} - \mathbf{b})^T(\mathbf{A}\mathbf{a} - \mathbf{b}) \tag{10}$$

Taking $\partial E / \partial a_I = 0, \forall I$, we have

$$\mathbf{A}^T\mathbf{A}\mathbf{a} = \mathbf{A}^T\mathbf{b} \tag{11}$$

In this test, we use MQ RBF as the approximation function, and choose $N_c = 4N_s$. To assess the errors of RBF approximation, we calculate the following error norms

$$e_{L_2} = \left(\int_\Omega (u - u^h)^2 dx \right)^{1/2} \tag{12}$$

$$e_{H^k} = \left(\int_\Omega \left(\frac{d^k}{dx^k}u - \frac{d^k}{dx^k}u^h \right)^2 dx \right)^{1/2}, k = 1 \sim 4 \tag{13}$$

where e_{L_2} is the L_2 error norm used to measure the error of u^h, and e_{H^k} is the H^k seminorm used to measure the errors of the derivatives of u^h. Since beam equations include up to 4th order derivatives in space, we calculate the errors in L_2 - and H^k - norms, $k = 1 \sim 4$, as shown in Fig. 2. The results clearly show the exponential convergence behavior, where the convergence rates are much higher than the algebraic convergence rates commonly observed in the conventional finite element

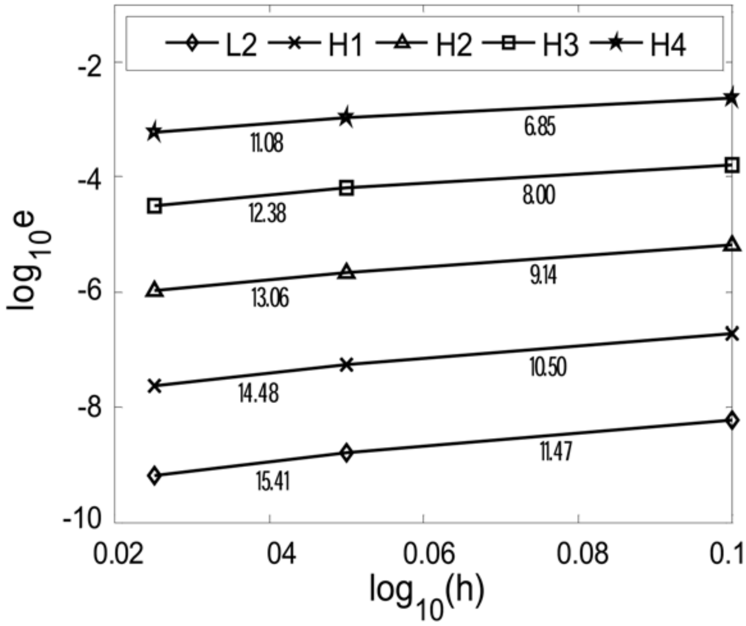

Fig. 2 Convergence rates for the errors of approximated sine function in L_2 - and H^k - norms (numbers showing the convergence rates)

methods. The results also show that the convergence rate reduces for approximation of higher order derivatives, which is consistent with the theory (Madych and Nelson 1992).

3. Radial basis collocation method for structural dynamics

3.1 Basic equations

Consider a general structural dynamic problem of the following strong form

$$\mathbf{A}\ddot{\mathbf{u}}(\mathbf{x},t)+\mathbf{S}\dot{\mathbf{u}}(\mathbf{x},t)+\mathbf{L}\mathbf{u}(\mathbf{x},t) = \mathbf{b}(\mathbf{x},t), \quad \text{in } \Omega\times[0,\tau] \tag{14}$$

with boundary conditions

$$\mathbf{B}^h\mathbf{u}(\mathbf{x},t) = \mathbf{h}(\mathbf{x},t), \quad \text{on } \partial\Omega^h\times[0,\tau] \tag{15}$$

$$\mathbf{B}^g\mathbf{u}(\mathbf{x},t) = \mathbf{g}(\mathbf{x},t), \quad \text{on } \partial\Omega^g\times[0,\tau] \tag{16}$$

and the initial conditions

$$\mathbf{u}(\mathbf{x},0) = \mathbf{u}_0(\mathbf{x}) \quad \text{in } \bar{\Omega}, \tag{17}$$

$$\dot{\mathbf{u}}(\mathbf{x},0) = \mathbf{v}_0(\mathbf{x}) \quad \text{in } \bar{\Omega}, \tag{18}$$

Here, $t\in[0,\tau]$, $\tau>0$, Ω is an open domain, $\partial\Omega^h$ is the Neumann boundary, $\partial\Omega^g$ is the Dirichlet boundary, $\overline{\Omega} = \Omega \cup \partial\Omega^h \cup \partial\Omega^g$, $\mathbf{A}$, $\mathbf{S}$ and $\mathbf{L}$ are the differential operators in Ω, $\mathbf{B}^h$ is the boundary operator on $\partial\Omega^h$, $\mathbf{B}^g$ is the boundary operator on $\partial\Omega^g$, $\mathbf{b}$ is the body force vector, $\mathbf{h}$ is the surface traction vector on $\partial\Omega^h$, $\mathbf{g}$ is the prescribed boundary displacement vector on $\partial\Omega^g$, $\mathbf{u}_0$ is the initial displacement vector, and $\mathbf{v}_0$ is the initial velocity vector.

For three-dimension, the solution $\mathbf{u} = [u_1, u_2, u_3]^T$ can be approximated as

$$\mathbf{u} \approx \mathbf{u}^h = \mathbf{\Phi}^{\mathrm{T}}\mathbf{d} \tag{19}$$

where

$$\mathbf{\Phi}^{\mathrm{T}} = (\mathbf{\Phi}_1\mathbf{\Phi}_2\ldots\mathbf{\Phi}_{N_s}),\ \mathbf{\Phi}_I = g_I(\mathbf{x})\mathbf{I},\ \mathbf{d} = (\mathbf{d}_1^{\mathrm{T}}\mathbf{d}_2^{\mathrm{T}}\ldots\mathbf{d}_{N_s}^{\mathrm{T}})^{\mathrm{T}},\ \mathbf{d}_I^{\mathrm{T}} = (\mathbf{d}_{1I}, \mathbf{d}_{2I}, \mathbf{d}_{3I}) \tag{20}$$

and $g_I(\mathbf{x})$ is the RBF with source point $\mathbf{x}_I \in \overline{\Omega}$.

3.2 Collocation method

Let $\mathbf{P}$ be a set of N_p collocation points in the domain Ω, $\mathbf{Q}$ be a set of N_q collocation points on the Neumann boundary $\partial\Omega^h$, and $\mathbf{R}$ be a set of N_r collocation points on the Dirichlet boundary $\partial\Omega^g$ as shown below

$$\mathbf{P} = \{\mathbf{p}_1, \mathbf{p}_2, \ldots, \mathbf{p}_{\mathrm{N_p}}\} \subseteq \Omega,\ \mathbf{Q} = \{\mathbf{q}_1, \mathbf{q}_2, \ldots, \mathbf{q}_{\mathrm{N_q}}\} \subseteq \partial\Omega^h,\ \mathbf{R} = \{\mathbf{r}_1, \mathbf{r}_2, \ldots, \mathbf{r}_{\mathrm{N_r}}\} \subseteq \partial\Omega^g \tag{21}$$

By introducing the approximation (19) into strong form (14) - (16), and evaluating the strong forms at the collocation points in the domain and on the boundaries, we have the following semi-discrete equation

$$\begin{bmatrix}\mathbf{M}\\ \mathbf{0}\\ \mathbf{0}\end{bmatrix}\ddot{\mathbf{d}} + \begin{bmatrix}\mathbf{C}\\ \mathbf{0}\\ \mathbf{0}\end{bmatrix}\dot{\mathbf{d}} + \begin{bmatrix}\mathbf{K}_1\\ \mathbf{K}_2\\ \mathbf{K}_3\end{bmatrix}\mathbf{d} = \begin{bmatrix}\mathbf{f}_1\\ \mathbf{f}_2\\ \mathbf{f}_3\end{bmatrix} \tag{22}$$

where

$$\mathbf{M} = \begin{bmatrix}\mathbf{A\Phi}^{\mathrm{T}}\ (\mathbf{p}_1)\\ \mathbf{A\Phi}^{\mathrm{T}}\ (\mathbf{p}_2)\\ \vdots\\ \mathbf{A\Phi}^{\mathrm{T}}\ (\mathbf{p}_{N_p})\end{bmatrix},\ \mathbf{C} = \begin{bmatrix}\mathbf{S\Phi}^{\mathrm{T}}\ (\mathbf{p}_1)\\ \mathbf{S\Phi}^{\mathrm{T}}\ (\mathbf{p}_2)\\ \vdots\\ \mathbf{S\Phi}^{\mathrm{T}}\ (\mathbf{p}_{N_p})\end{bmatrix} \tag{23}$$

$$\mathbf{K}_1 = \begin{bmatrix}\mathbf{L\Phi}^{\mathrm{T}}\ (\mathbf{p}_1)\\ \mathbf{L\Phi}^{\mathrm{T}}\ (\mathbf{p}_2)\\ \vdots\\ \mathbf{L\Phi}^{\mathrm{T}}\ (\mathbf{p}_{N_p})\end{bmatrix},\ \mathbf{K}_2 = \begin{bmatrix}\mathbf{B}^h\mathbf{\Phi}^{\mathrm{T}}\ (\mathbf{q}_1)\\ \mathbf{B}^h\mathbf{\Phi}^{\mathrm{T}}\ (\mathbf{q}_2)\\ \vdots\\ \mathbf{B}^h\mathbf{\Phi}^{\mathrm{T}}\ (\mathbf{q}_{N_q})\end{bmatrix},\ \mathbf{K}_3 = \begin{bmatrix}\mathbf{B}^g\mathbf{\Phi}^{\mathrm{T}}\ (\mathbf{r}_1)\\ \mathbf{B}^g\mathbf{\Phi}^{\mathrm{T}}\ (\mathbf{r}_2)\\ \vdots\\ \mathbf{B}^g\mathbf{\Phi}^{\mathrm{T}}\ (\mathbf{r}_{N_r})\end{bmatrix} \tag{24}$$

$$\mathbf{f}_1 = \begin{bmatrix} \mathbf{b}(\mathbf{p}_1, t) \\ \mathbf{b}(\mathbf{p}_2, t) \\ \vdots \\ \mathbf{b}(\mathbf{p}_{N_p}, t) \end{bmatrix}, \mathbf{f}_2 = \begin{bmatrix} \mathbf{h}(\mathbf{q}_1, t) \\ \mathbf{h}(\mathbf{q}_2, t) \\ \vdots \\ \mathbf{h}(\mathbf{q}_{N_q}, t) \end{bmatrix}, \mathbf{f}_3 = \begin{bmatrix} \mathbf{g}(\mathbf{r}_1, t) \\ \mathbf{g}(\mathbf{r}_2, t) \\ \vdots \\ \mathbf{g}(\mathbf{r}_{N_r}, t) \end{bmatrix} \tag{25}$$

Here $\mathbf{M}$, $\mathbf{C}$, and $\mathbf{K}_1$ are the matrices associated with differential operators $\mathbf{A}$, $\mathbf{S}$, and $\mathbf{L}$, respectively, and $\mathbf{K}_2$ and $\mathbf{K}_3$ are associated with Neumann boundary operator $\mathbf{B}^h$ and Dirichlet boundary operator $\mathbf{B}^g$, respectively.

Evaluating initial conditions (17)-(18) at all the collocation points in the domain and on the boundaries yields

$$\mathbf{H}\mathbf{d}(0): = \begin{bmatrix} \mathbf{H}_1 \\ \mathbf{H}_2 \\ \mathbf{H}_3 \end{bmatrix} \mathbf{d}(0) = \begin{bmatrix} \bar{\mathbf{u}}_1 \\ \bar{\mathbf{u}}_2 \\ \bar{\mathbf{u}}_3 \end{bmatrix} = :\bar{\mathbf{u}} \tag{26}$$

$$\mathbf{H}\dot{\mathbf{d}}(0): = \begin{bmatrix} \mathbf{H}_1 \\ \mathbf{H}_2 \\ \mathbf{H}_3 \end{bmatrix} \dot{\mathbf{d}}(0) = \begin{bmatrix} \bar{\mathbf{v}}_1 \\ \bar{\mathbf{v}}_2 \\ \bar{\mathbf{v}}_3 \end{bmatrix} = :\bar{\mathbf{v}} \tag{27}$$

where

$$\mathbf{H}_1 = \begin{bmatrix} \mathbf{\Phi}^{\mathrm{T}}(\mathbf{p}_1) \\ \mathbf{\Phi}^{\mathrm{T}}(\mathbf{p}_2) \\ \vdots \\ \mathbf{\Phi}^{\mathrm{T}}(\mathbf{p}_{N_p}) \end{bmatrix}, \mathbf{H}_2 = \begin{bmatrix} \mathbf{\Phi}^{\mathrm{T}}(\mathbf{q}_1) \\ \mathbf{\Phi}^{\mathrm{T}}(\mathbf{q}_2) \\ \vdots \\ \mathbf{\Phi}^{\mathrm{T}}(\mathbf{q}_{N_q}) \end{bmatrix}, \mathbf{H}_3 = \begin{bmatrix} \mathbf{\Phi}^{\mathrm{T}}(\mathbf{r}_1) \\ \mathbf{\Phi}^{\mathrm{T}}(\mathbf{r}_2) \\ \vdots \\ \mathbf{\Phi}^{\mathrm{T}}(\mathbf{r}_{N_r}) \end{bmatrix} \tag{28}$$

$$\bar{\mathbf{u}}_1 = \begin{bmatrix} \mathbf{u}_0(\mathbf{p}_1) \\ \mathbf{u}_0(\mathbf{p}_2) \\ \vdots \\ \mathbf{u}_0(\mathbf{p}_{N_p}) \end{bmatrix}, \bar{\mathbf{u}}_2 = \begin{bmatrix} \mathbf{u}_0(\mathbf{q}_1) \\ \mathbf{u}_0(\mathbf{q}_2) \\ \vdots \\ \mathbf{u}_0(\mathbf{q}_{N_q}) \end{bmatrix}, \bar{\mathbf{u}}_3 = \begin{bmatrix} \mathbf{u}_0(\mathbf{r}_1) \\ \mathbf{u}_0(\mathbf{r}_2) \\ \vdots \\ \mathbf{u}_0(\mathbf{r}_{N_r}) \end{bmatrix} \tag{29}$$

$$\bar{\mathbf{v}}_1 = \begin{bmatrix} \mathbf{v}_0(\mathbf{p}_1) \\ \mathbf{v}_0(\mathbf{p}_2) \\ \vdots \\ \mathbf{v}_0(\mathbf{p}_{N_p}) \end{bmatrix}, \bar{\mathbf{v}}_2 = \begin{bmatrix} \mathbf{v}_0(\mathbf{q}_1) \\ \mathbf{v}_0(\mathbf{q}_2) \\ \vdots \\ \mathbf{v}_0(\mathbf{q}_{N_q}) \end{bmatrix}, \bar{\mathbf{v}}_3 = \begin{bmatrix} \mathbf{v}_0(\mathbf{r}_1) \\ \mathbf{v}_0(\mathbf{r}_2) \\ \vdots \\ \mathbf{v}_0(\mathbf{r}_{N_r}) \end{bmatrix} \tag{30}$$

By imposing the boundary conditions in the last 2 equations of Eq. (22) by a static condensation, we have

$$\hat{\mathbf{M}}\ddot{\hat{\mathbf{d}}} + \hat{\mathbf{C}}\dot{\hat{\mathbf{d}}} + \hat{\mathbf{K}}\hat{\mathbf{d}} = \hat{\mathbf{f}} \tag{31}$$

where $\hat{\mathbf{M}}$, $\hat{\mathbf{C}}$, $\hat{\mathbf{K}}$, and $\hat{\mathbf{f}}$ are the statically condensed matrices and vector associated with the matrices **M**, **C**, **K**, and **f**, respectively, by imposing the boundary conditions, and the vector $\hat{\mathbf{d}}$, $\dot{\hat{\mathbf{d}}}$, and $\ddot{\hat{\mathbf{d}}}$ contain the independent variables of $\mathbf{d}$, $\dot{\mathbf{d}}$, and $\ddot{\mathbf{d}}$, respectively. The construction of the statically condensed semi-discrete equation in (31) follows the static condensation procedure in Appendix A.

The initially conditions can also be statically condensed by imposing the boundary conditions to yield

$$\hat{\mathbf{H}}\hat{\mathbf{d}}(0) = \hat{\mathbf{u}} \tag{32}$$

$$\hat{\mathbf{H}}\dot{\hat{\mathbf{d}}}(0) = \hat{\mathbf{v}} \tag{33}$$

where $\hat{\mathbf{H}}$, $\hat{\mathbf{u}}$, and $\hat{\mathbf{v}}$ are the statically condensed forms of $\mathbf{H}$, $\bar{\mathbf{u}}$, and $\bar{\mathbf{v}}$, respectively.

3.3. Time integration and full discrete equation

The temporal discretization of (31) can be expressed as:

$$\hat{\mathbf{M}}\hat{\mathbf{a}}_{n+1} + \hat{\mathbf{C}}\hat{\mathbf{v}}_{n+1} + \hat{\mathbf{K}}\hat{\mathbf{d}}_{n+1} = \hat{\mathbf{f}}_{n+1} \tag{34}$$

where $\hat{\mathbf{d}}_{n+1}$, $\hat{\mathbf{v}}_{n+1}$ and $\hat{\mathbf{a}}_{n+1}$ are the approximation of $\hat{\mathbf{d}}(t_{n+1})$, $\dot{\hat{\mathbf{d}}}(t_{n+1})$ and $\ddot{\hat{\mathbf{d}}}(t_{n+1})$, respectively, and n is the time step counter. Further considering Newmark method for the time integration, we have

$$\hat{\mathbf{d}}_{n+1} = \tilde{\mathbf{d}}_{n+1} + \beta\Delta t^2\hat{\mathbf{a}}_{n+1} \tag{35}$$

$$\hat{\mathbf{v}}_{n+1} = \tilde{\mathbf{v}}_{n+1} + \gamma\Delta t\hat{\mathbf{a}}_{n+1} \tag{36}$$

where $\tilde{\mathbf{d}}_{n+1}$ and $\tilde{\mathbf{v}}_{n+1}$ are the predictors defined as

$$\tilde{\mathbf{d}}_{n+1} = \hat{\mathbf{d}}_n + \Delta t\tilde{\mathbf{v}}_n + \frac{1}{2}(1-2\beta)\Delta t^2\hat{\mathbf{a}}_n \tag{37}$$

$$\tilde{\mathbf{v}}_{n+1} = \tilde{\mathbf{v}}_n + (1-\gamma)\Delta t\hat{\mathbf{a}}_n \tag{38}$$

and β and γ are the time integration parameters. Introducing Eqs. (35) and (36) into (34) yields the following equation

$$\mathbf{M}^*\mathbf{a}_{n+1} = \mathbf{f}^*_{n+1} \tag{39}$$

where

$$\mathbf{M}^* = \hat{\mathbf{M}} + \gamma\Delta t\hat{\mathbf{C}} + \beta\Delta t^2\hat{\mathbf{K}},\ \mathbf{f}^*_{n+1} = \hat{\mathbf{f}}_{n+1} - \hat{\mathbf{K}}\tilde{\mathbf{d}}_{n+1} - \hat{\mathbf{C}}\tilde{\mathbf{v}}_{n+1} \tag{40}$$

Eq. (39) is an over-determined system, and least-squares method as discussed in (9)-(11) is used to obtain acceleration $\mathbf{a}_{n+1}$.

4. SC-RBCM for dynamic analysis of moving beams

4.1 Difficulty in RBCM for analysis of dynamic beam problems

We first consider a beam without axial movement using the radial basis collocation method (RBCM) discussed in Section 3. The free vibration equation of a simply supported beam (SSB) is

$$EIu_{xxxx} + mu_{tt} = 0, \qquad 0 < x < L \tag{41}$$

where m is the mass per length, EI is the bending stiffness, L is the span of the beam, and $u\,(x,\,t)$ is the deflection. The following non-dimensional variables are introduced

$$\tilde{x} = \frac{x}{L}, \tilde{u} = \frac{u}{L}, \tilde{t} = t\sqrt{\frac{EI}{mL^4}} \tag{42}$$

Substituting (42) into (41) and dropping the superpose "~" for notational simplicity, we have the dimensionless equation

$$u_{xxxx} + u_{tt} = 0, \qquad 0 < x < 1 \tag{43}$$

The boundary and initial conditions are given as

$$u(0, t) = 0, u_{xx}(0, t) = 0, u(1, t) = 0, u_{xx}(1, t) = 0 \tag{44}$$

$$u(x, 0) = 0, \dot{u}(x, 0) = v_0 \sin(\pi x) \tag{45}$$

where $v_0 = 0.01$. The analytical solutions can be found in Clough and Penzien (2003). We introduce the approximation of unknown u by RBF as

$$u^h(x, t) = \sum_{I=1}^{N_s} g_I(x) d_I(t) \tag{46}$$

where $g_I\,(x)$ is the one-dimensional MQ RBF, N_s is the number of source points and $d_I\,(t)$ is the expansion coefficient. Evaluating strong forms at the N_c collocation points renders the following semi-discretize equation

$$\begin{bmatrix} 0 & 0 & \cdots & 0 \\ 0 & 0 & \cdots & 0 \\ g_1(\hat{x}_2) & g_2(\hat{x}_2) & \cdots & g_{N_s}(\hat{x}_2) \\ \vdots & \vdots & \ddots & \vdots \\ g_1(\hat{x}_{N_c-1}) & g_2(\hat{x}_{N_c-1}) & \cdots & g_{N_s}(\hat{x}_{N_c-1}) \\ 0 & 0 & \cdots & 0 \\ 0 & 0 & \cdots & 0 \end{bmatrix} \ddot{\mathbf{d}}(t)$$

$$+\begin{bmatrix} g_1(\hat{x}_1) & g_2(\hat{x}_1) & \cdots & g_{N_s}(\hat{x}_1) \\ g_{1,xx}(\hat{x}_1) & g_{2,xx}(\hat{x}_1) & \cdots & g_{N_s,xx}(\hat{x}_1) \\ g_{1,xxxx}(\hat{x}_2) & g_{2,xxxx}(\hat{x}_2) & \cdots & g_{N_s,xxxx}(\hat{x}_2) \\ \vdots & \vdots & \ddots & \vdots \\ g_{1,xxxx}(\hat{x}_{N_c-1}) & g_{2,xxxx}(\hat{x}_{N_c-1}) & \cdots & g_{N_s,xxxx}(\hat{x}_{N_c-1}) \\ g_{1,xx}(\hat{x}_{N_c}) & g_{2,xx}(\hat{x}_{N_c}) & \cdots & g_{N_s,xx}(\hat{x}_{N_c}) \\ g_1(\hat{x}_{N_c}) & g_2(\hat{x}_{N_c}) & \cdots & g_{N_s}(\hat{x}_{N_c}) \end{bmatrix} \mathbf{d}(t) = \mathbf{0} \tag{47}$$

The first two and last two equations in (47) are associated with the four boundary conditions, and the rest of $N_c - 4$ equations are associated with the collocation of the differential equation. For desired accuracy and convergence, the number of collocation points N_c needs to be greater than the number of source points N_s, and the numerical studies in Hu *et al.* (2007) suggested that $N_c \approx 4N_s$ yields good accuracy. This treatment of collocation yields an over-determined system and is solved by least-squares method. In this test, $N_s = 11$, $N_c = 41$, shape parameter $c = 0.6$, time integration parameters $\beta = 0, \gamma = 1/2$, and time step $\Delta t = 0.0005$ are used.

We first consider the case of imposing boundary conditions by a direct collocation at the boundary points as shown in (22) for general problem, and using (47) for this example. The errors of boundary solutions obtained from this approach are of the level 10^{-3} as shown in Fig. 3 and Fig. 4. The consequence of these boundary errors is demonstrated in Fig. 5 where significant errors in the midpoint of the domain are induced regardless of spatial refinement. As have been discussed in Hu *et al.* (2007), proper weights applied to the boundary collocation equations can significantly enhance the solution accuracy. This approach is introduced to (22) and yields:

$$\begin{bmatrix} \mathbf{M} \\ \mathbf{0} \\ \mathbf{0} \end{bmatrix} \ddot{\mathbf{d}} + \begin{bmatrix} \mathbf{C} \\ \mathbf{0} \\ \mathbf{0} \end{bmatrix} \dot{\mathbf{d}} + \begin{bmatrix} \mathbf{K}_1 \\ \sqrt{w_h}\mathbf{K}_2 \\ \sqrt{w_g}\mathbf{K}_3 \end{bmatrix} \mathbf{d} = \begin{bmatrix} \mathbf{f}_1 \\ \sqrt{w_h}\mathbf{f}_2 \\ \sqrt{w_g}\mathbf{f}_3 \end{bmatrix} \tag{48}$$

where $\sqrt{w_h}$ and $\sqrt{w_g}$ are the weights associated with the Neumann and Dirichlet boundary conditions, respectively. The same approach can be easily applied to (47). Optimal weights have been recommended in Hu *et al.* (2007) for static problems, and for this dynamic problem we numerically test different weights with $\sqrt{w_g} = \sqrt{w_h} \equiv \sqrt{w}$ as shown in Fig. 6 and Fig. 7. The results show that the boundary weights do not improve the solution accuracy in this dynamic problem.

We then consider a statically condensed semi-discrete equation in (31)-(33) following Appendix A before performing temporal discretization and least-squares solution procedures. The numerical solutions displayed in Figs. 8 (a)-(c) indicate that the statically condensed RBCM (SC-RBCM) not only yields better boundary solutions (as expected), it also greatly improves the solutions inside the domain compared to the standard RBCM with weighted boundary collocation equations.

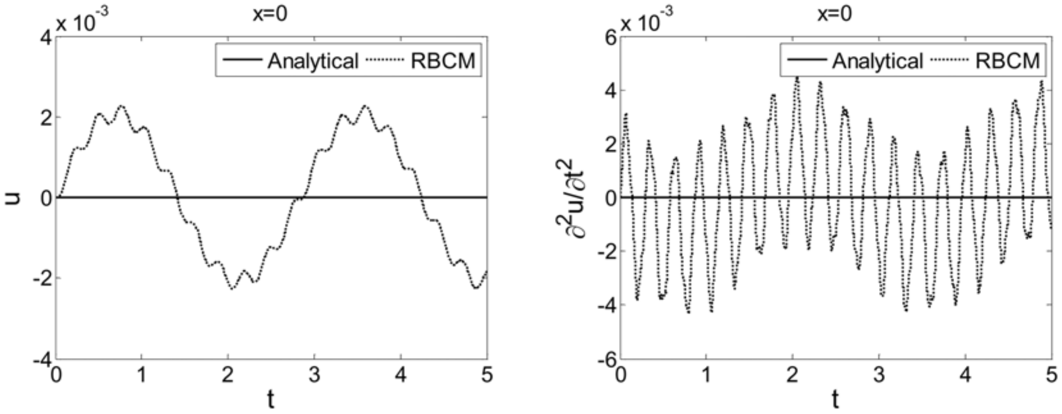

Fig. 3 Boundary solutions of the SSB at $x = 0$

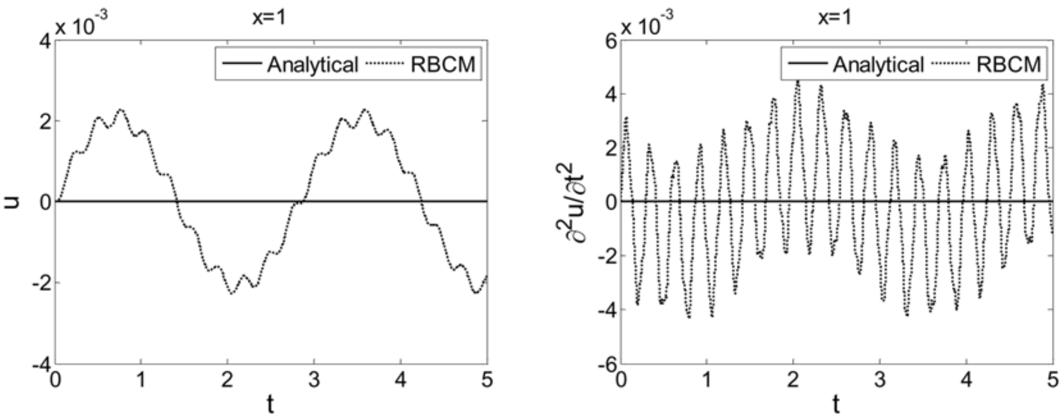

Fig. 4 Boundary solutions of the SSB at $x = 1$

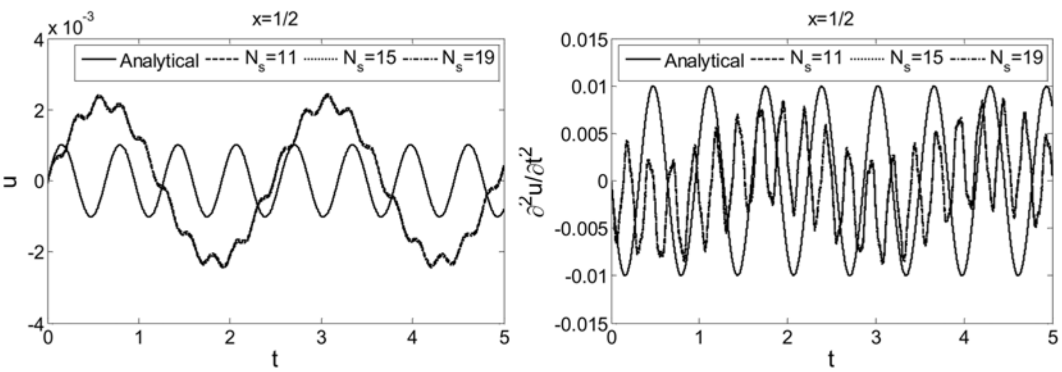

Fig. 5 Numerical solutions of the SSB at $x = 1 / 2$ with different discretizations

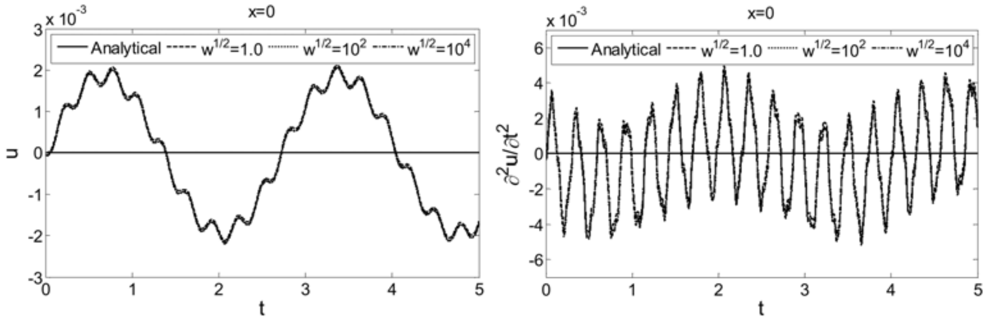

Fig. 6 Numerical solutions of the SSB at $x = 0$ with different weights applied to the boundary collocation equations

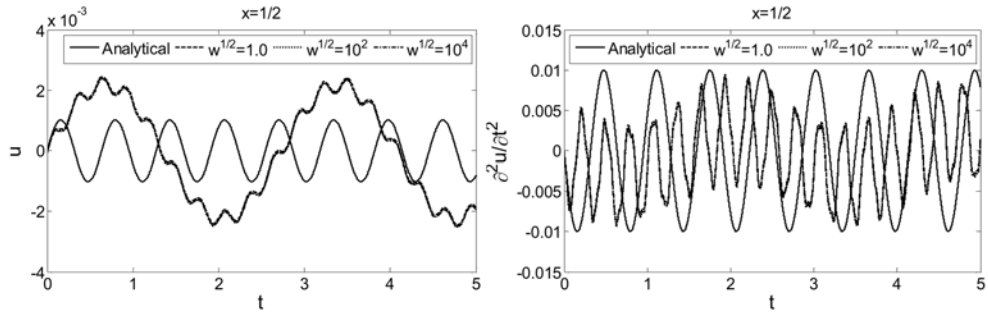

Fig. 7 Numerical solutions of the SSB at $x = 1/2$ with different weights applied to the boundary collocation equations

4.2. Axially moving simply supported beam

The governing equation of an axially moving simply supported beam is given as (Wickert and Mote 1991)

$$\rho u_{tt} + 2\rho v u_{xt} - (P - \rho v^2) u_{xx} + EI u_{xxxx} = 0, 0 < x < L \tag{49}$$

where ρ is the mass density, $u(x, t)$ is the transverse displacement, v is the axial translation velocity, P is the axial tension, and EI is the bending stiffness. The equation of motion can be degenerated into the beam dynamic equation in (41) with zero axial movement and axial tension (i.e. $v = 0$, $P = 0$).

The following non-dimensional variables are introduced

$$\tilde{x} = \frac{x}{L}, \tilde{u} = \frac{u}{L}, \tilde{t} = t\sqrt{\frac{P}{\rho L^2}}, \tilde{v} = v\sqrt{\frac{\rho}{P}}, \text{ and } \xi = \frac{EI}{PL^2} \tag{50}$$

Substituting (50) into (49) gives the dimensionless equation (dropping the superposed "~" for dimensional simplicity)

$$u_{tt} + 2v u_{xt} - (1 - v^2) u_{xx} + \xi u_{xxxx} = 0, 0 < x < 1 \tag{51}$$

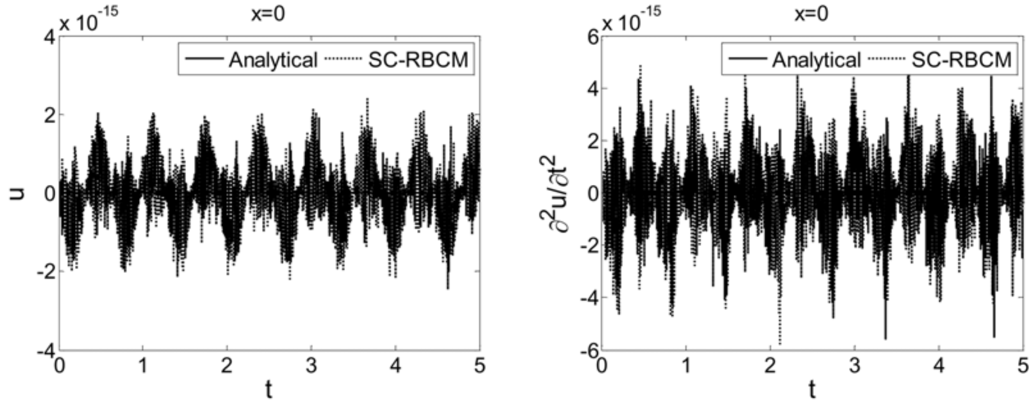

Fig. 8(a) Numerical solutions of the SSB at $x = 0$ obtained from SC-RBCM

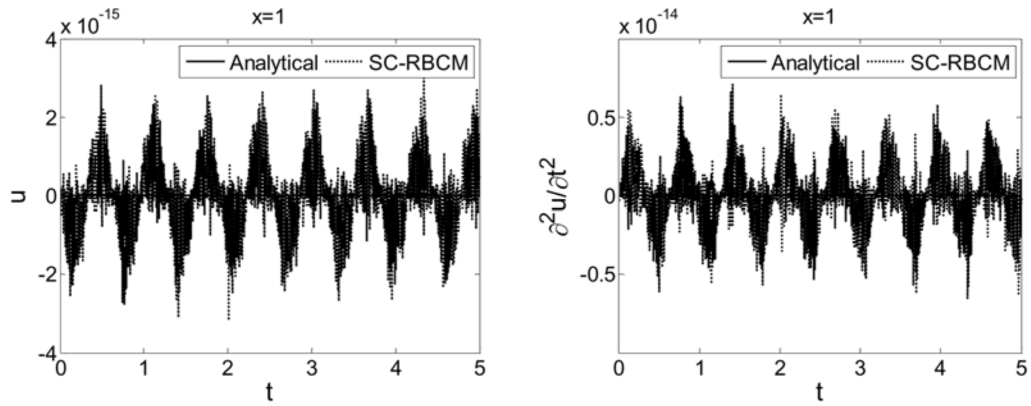

Fig. 8(b) Numerical solutions of the SSB at $x = 1$ obtained from SC-RBCM

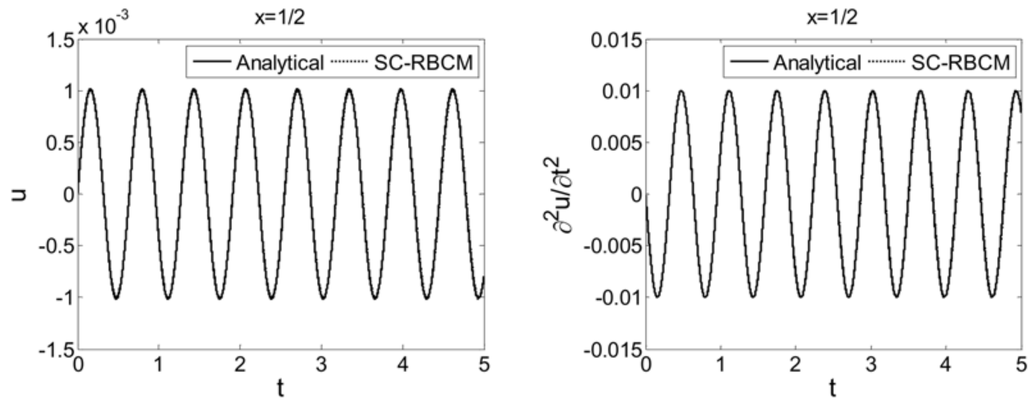

Fig. 8(c) Numerical solutions of the SSB at the midpoint obtained from SC-RBCM

The boundary and initial conditions are

$$u(0,t) = 0, EIu_{xx}(0,t) = 0, u(1,t) = 0, EIu_{xx}(1,t) = 0 \tag{52}$$

$$u(x,0) = 0, \dot{u}(x,0) = v_0 \sin(\pi x) \tag{53}$$

where $v_0 = 0.01$.

Corresponding to (14)-(16), we have

$$\mathbf{A} = 1, \mathbf{S} = 2v\frac{\partial}{\partial x}, \mathbf{L} = -(1-v^2)\frac{\partial^2}{\partial x^2} + \xi\frac{\partial^4}{\partial x^4}, \mathbf{b} = 0$$

$$\mathbf{B}_1^h = EI\frac{\partial^2}{\partial x^2}, \mathbf{B}_1^g = 1, \mathbf{B}_2^h = EI\frac{\partial^2}{\partial x^2}, \mathbf{B}_2^g = 1 \tag{54}$$

Analytical solutions from Kong and Parker (2003) are used for comparison with the numerical solutions. Figs. 9 (a)-(c) show that the proposed SC-RBCM generates good accuracy on the boundaries as well as in the domain. The results in Figs. 9 (a)-(c) also demonstrate that the transverse deflection increases and the natural frequencies decrease as the simply supported beam moves axially.

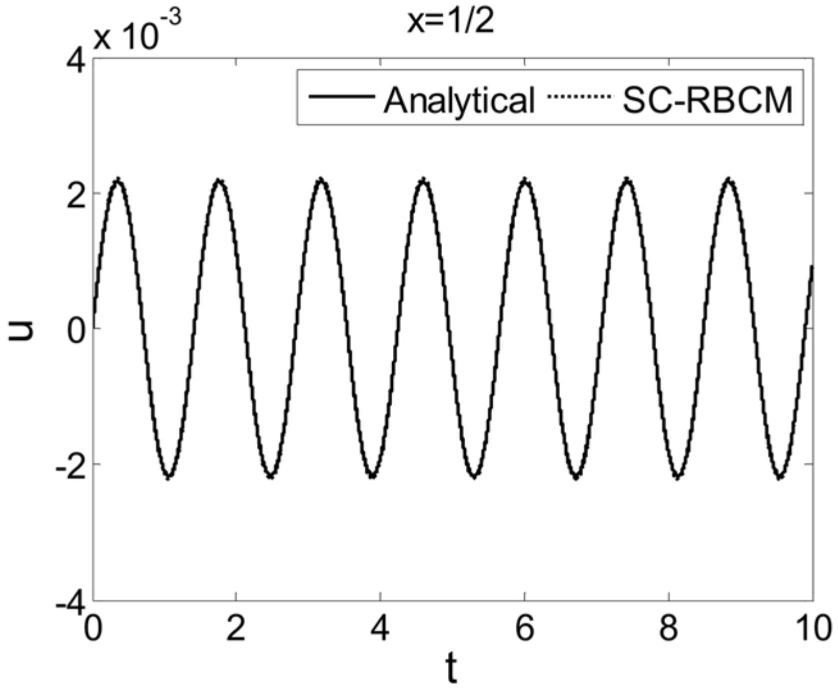

Fig. 9(a) Numerical solutions of the axially moving SSB obtained from SC-RBCM at the midpoint when $v = 0$, $\xi = 0.1$

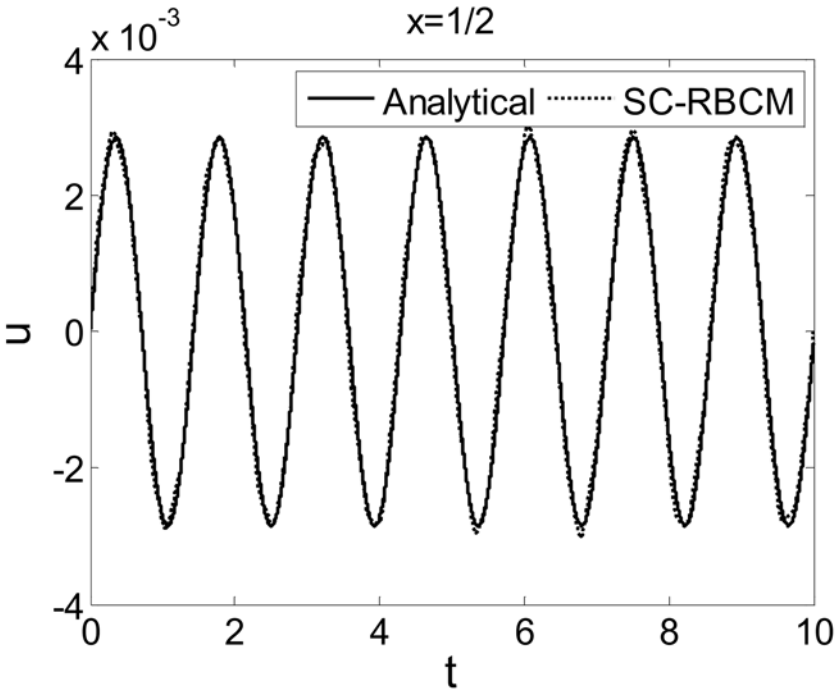

Fig. 9(b) Numerical solutions of the axially moving SSB obtained from SC-RBCM at the midpoint when $v = 0.15$, $\xi = 0.1$

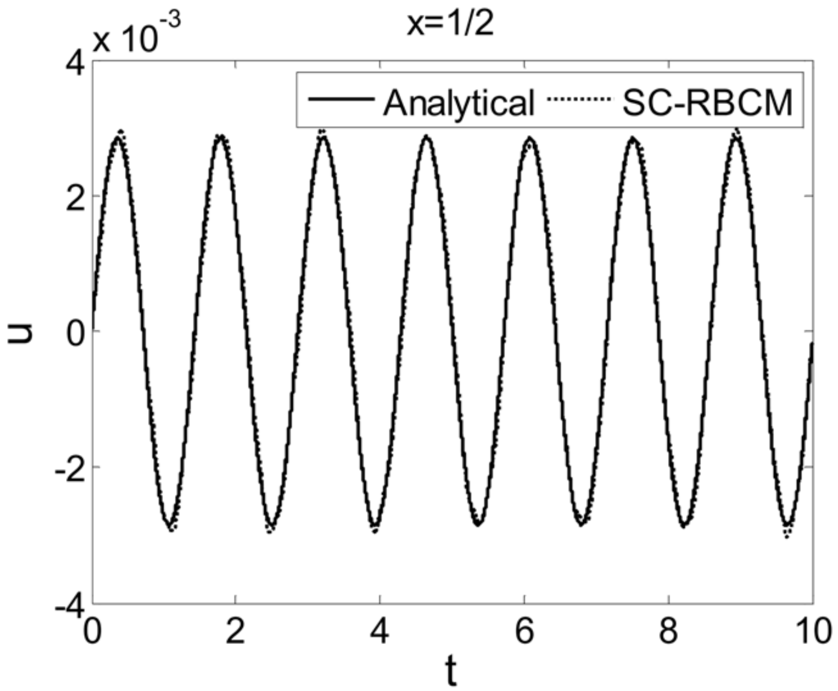

Fig. 9(c) Numerical solutions of the axially moving SSB obtained from SC-RBCM at the midpoint when $v = -0.15$, $\xi = 0.1$

4.3. Axially moving cantilever beam

The governing equation of an axially moving cantilever beam is given below (Wang *et al.* 2009)

$$\rho u_{tt} + 2\rho v u_{xt} + \rho(la - xa + v^2)u_{xx} + EIu_{xxxx} = 0, 0 < x < l(t), t \geq 0 \tag{55}$$

where ρ is the mass density, $u(x, t)$ is the transverse displacement, v is the axial translation speed, a is the translation acceleration, and EI is the bending stiffness. Introducing $\xi = \frac{EI}{\rho}$, (55) can be rewritten as

$$u_{tt} + 2v u_{xt} + (la - xa + v^2)u_{xx} + \xi u_{xxxx} = 0, 0 < x < l(t), t \geq 0 \tag{56}$$

The boundary conditions and initial conditions of this problem are

$$u(0, t) = 0, u_x(0, t) = 0, EIu_{xx}(l, t) = 0, EIu_{xxx}(l, t) = 0 \tag{57}$$

$$u(x, 0) = 0, \dot{u}(x, 0) = v_0\left\{\frac{1}{3}\left(\frac{x}{L}\right)^4 - \frac{4}{3}\left(\frac{x}{L}\right)^3 + 2\left(\frac{x}{L}\right)^2\right\} \tag{58}$$

where $v_0 = 0.01$. Corresponding to (14)-(16), we have

$$\mathbf{A} = 1, \mathbf{S} = 2v\frac{\partial}{\partial x}, \mathbf{L} = (la - xa + v^2)\frac{\partial^2}{\partial x^2} + \xi\frac{\partial^4}{\partial x^4}, \mathbf{b} = 0$$

$$\mathbf{B}_I^h = EI\frac{\partial^2}{\partial x^2}, \mathbf{B}_2^h = EI\frac{\partial^3}{\partial x^3}, \mathbf{B}_I^g = 1, \mathbf{B}_2^g = EI\frac{\partial}{\partial x} \tag{59}$$

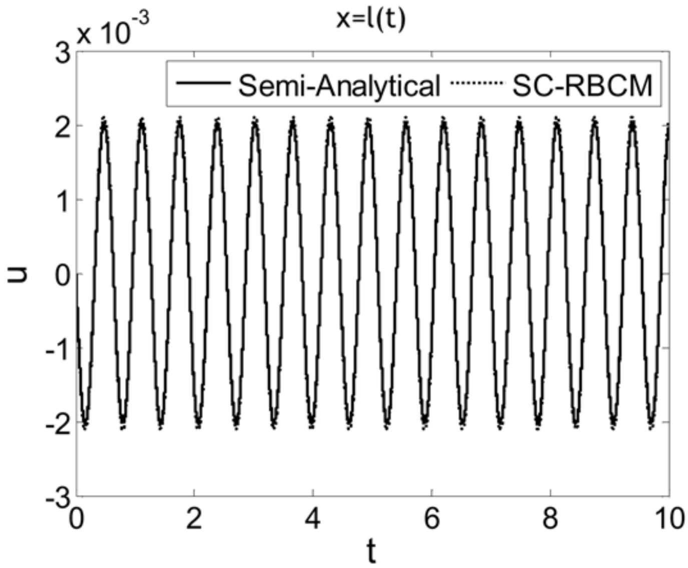

Fig. 10(a) Numerical solutions of the axially moving CB obtained from SC-RBCM at $x = l(t)$ with translation velocities $v = 0$, $\xi = 1.0$, $l(0) = 1.0$

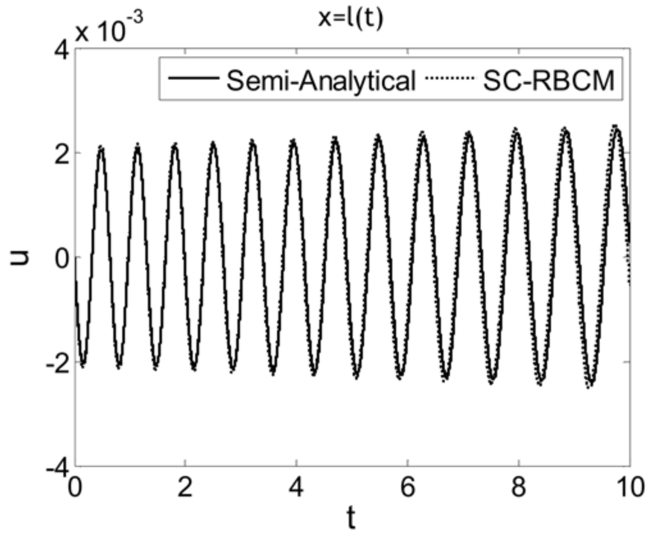

Fig. 10(b) Numerical solutions of the axially moving CB obtained from SC-RBCM at $x = l\,(t)$ with translation velocities $v = 0.01$, $\xi = 1.0$, $l\,(0) = 1.0$

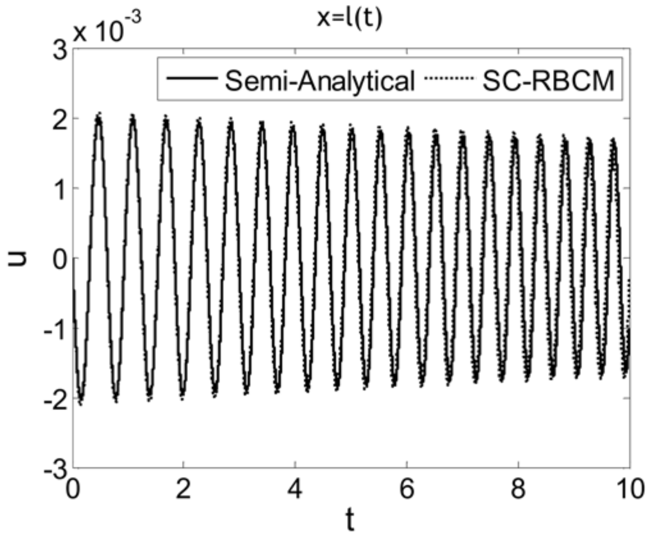

Fig. 10(c) Numerical solutions of the axially moving CB obtained from SC-RBCM at $x = l\,(t)$ with translation velocities $v = -0.01$, $\xi = 1.0$, $l\,(0) = 1.0$

The semi-analytical solutions by Wang *et al*. (2009) are used to compare with the numerical solutions. The results shown in Figs. 10 (a)-(c) again demonstrate that SC-RBCM yields good accuracy for the axially moving beam problems. As illustrated in the Fig. 10 (b), the deflection increases and the natural frequencies decrease during the beam extension ($v > 0$), which is due to the "softer" response as the beam length increases when the beam moves with positive velocity (Tadikonda and Baruh 1992). On the other hand, during the beam retraction ($v < 0$), the amplitude of deflection decreases and the frequencies increase as shown in Fig. 10 (c) and this is because the beam becomes “stiffer” as the length reduces (Tadikonda and Baruh 1992).

5. Conclusions

We introduced the radial basis collocation method (RBCM) to structural dynamics problem with specific consideration of axially moving beams. The governing equation for a beam involves a 4^{th} order spatial differentiation of the deflection, and this makes the employment of radial basis functions (RBFs) an attractive choice for spatial discretization owing to their infinite differentiability. Further, unlike other shape functions employed in the meshfree methods, such as the moving least-squares or the reproducing kernel approximations where the derivatives involve tedious algebraic expressions with matrix inversions, the derivatives of RBFs are considerably simple.

One of the advantages of RBCM for solving PDE is its straightforward treatment of Dirichlet and Neumann boundary conditions. These boundary conditions are evaluated at the boundary collocation points, and these boundary discrete equations are solved together with the equations associated with the evaluation of PDE at the domain collocation points by the least-squares method. However, it has been reported by Hu *et al*. (2007) that this imposition of boundary conditions yields large errors near the boundaries, and certain weights applied to the boundary collocation equations can significantly reduce the boundary errors. Those boundary weights have been obtained based on balancing the domain and boundary errors, and this method was called the weighted RBCM in Hu *et al*. (2007). In this study we found that although the weighted RBCM helps to reduce boundary errors, these errors propagate in space and time and generates significant errors in the domain interior in dynamic problems. We then introduced a simple static condensation to the semi-discrete equation associated with the boundary conditions, and perform time integration on the condensed semi-discrete equation and initial conditions. The results show a substantial improvement over the standard RBCM or weighted RBCM methods. The effectiveness of the proposed method was validated by several numerical examples of axially moving beam problems.

Acknowledgements

The support of this work by the National Natural Science Foundation of China (NSFC) under Project No. 10572104 to the first author, the US Army ERDC under contract W912HZ-07-C-0019 to the second author, and the National Science Council of Taiwan, R. O. C., under project number NSC 96-2115-M-029-002-MY2 to the third author are greatly acknowledged.

References

Chen, J.S., Hu, W. and Hu, H.Y. (2008), “Reproducing Kernel Enhanced Local Radial Basis Collocation Method”, Int. *J. Numer. Method. E.*, **75**, 600-627.

Chen, J.S., Wang, L., Hu, H.Y. and Chi, S.W. (2009), “Subdomain Radial Basis Collocation Method for Heterogeneous Media”, *J. Numer. Method. E.*, **80**, 163-190.

Clough, W.R. and Penzien, J. (2003), *Dynamics of Structures*, 3rd Edition, Computers and Structures, Inc..

Fasshauer, G.E. (1999), “Solving differential equations with radial basis functions: multilevel methods and smoothing”, *Mech. Adv. Mater. Struc.,* **11**(2/3), 139-159.

Ferreira, A.J.M. (2003), "Thick composite beam analysis using a global meshless approximation based on radial basis functions", *Mech. Adv. Mater. Struc.,* **10**, 271-284.

Gurgoze, M. (1999), "Transverse vibration of a flexible beam sliding through a prismatic joint", *J. Sound Vib.,* **223**(3), 467-482.

Hardy, R.L. (1971), "Multiquadric equations of topography and other irregular surfaces", *J. Geophys. Res.,* **176**, 1905-1915.

Hon, Y.C. and Schaback, R. (2001), "On unsymmetric collocation by radial basis functions", *Appl. Math. Comput.,* **119**(2-3), 177-186.

Hu, H.Y., Chen, J.S. and Hu, W. (2007), "Weighted radial basis collocation method for boundary value problems", *Int. J. Numer. Method. E.*, **69**, 2736-2757.

Kansa, E.J. (1990a), "Multiquadrics-a scattered data approximation scheme with applications to computational fluid-dynamics - i. surface approximations and partial derivative estimates", *Comput. Math. Appl.,* **19**, 127-145.

Kansa, E.J. (1990b), "Multiquadrics-a scattered data approximation scheme with applications to computational fluid-dynamics - ii. solutions to parabolic, hyperbolic and elliptic partial differential equations", *Comput. Math. Appl.,* **19**, 147-161.

Kong, L. and Parker, R.G. (2004), "Approximate eigensolutions of axially moving beams with small flexural stiffness", *J. Sound Vib.,* **276**, 459-469.

Lee, U. and Jang, I. (2007), "On the boundary for axially moving beams", *J. Sound Vib.,* **306**, 675-690.

Lee, U. and Oh, H. (2005), "Dynamics of an axially moving viscoelastic beam subject to axial tension", *Int. J. Solids Struct.,* **42**, 2381-2398.

Liu, Y., Liew, K.M., Hon, Y.C. and Zhang, X. (2005), "Numerical simulation and analysis of an electroactuated beam using a radial basis function", *Smart Mater. Struct.,* **14**, 1163-1171.

Madych, W.R. and Nelson, S.A. (1992), "Bounds on multivariate polynomials and exponential error estimates for multiquadric interpolation", *J. Approx. Theory,* **70**, 94-114.

Ozkaya, E. and Pakdemirli, M. (2002), "Group-theoretic approach to axially accelerating beam problem", *Acta Mech.,* **155**, 111-123.

Raju, I.S., Phillips, D.R. and Krishnamurthy, T. (2003), "Meshless local Petrov-Galerkin Euler-Bernoulli beam problems: a radial basis function approach", *Proceedings of the 44th AIAA/ASME/AHS Structure, Structure Dynamics, and Materials Conference*, Norfolk, April.

Rao, G.V. (1992), "Linear dynamics and active control of an elastically supported traveling string", *Comput. Struct.,* **43**(6), 1041-1049.

Stylianou, M. and Tabarrok, B. (1994), "Finite element analysis of an axially moving beam, part I: time integration", *J. Sound Vib.,* **178**(4), 433-453.

Sylla, M. and Asseke, B. (2008), "Dynamics of a rotating flexible and symmetric spacecraft using impedance matrix in terms of the flexible appendages cantilever modes", *Multibody Syst. Dyn.,* **19**, 345-364.

Tadikonda, S.S.K. and Baruh, H. (1992), "Dynamics and control of a translating flexible beam with a prismatic joint", *J. Dyn. Syst-T. ASME,* **114**(3), 422-427.

Tiago, C.M. and Leitao, V.M.A. (2006), "Application of radial basis functions to linear and nonlinear structural analysis problems", *Comput. Math. Appl.,* **51**, 1311-1334.

Wang, L.H., Hu, Z.D., Zhong, Z. and Ju, J.W. (2009), "Hamiltonian dynamic analysis of an axially translating beam featuring time-variant velocity", *Acta Mech.,* **206**(3-4), 149-161.

Wickert, J.A. and Mote, C.D., Jr. (1991), "Response and discretization methods for axially moving materials", Appl. Mech. Rev., **44**(11S), 279-284.

Wu, L.Y., Chung, L.L. and Huang, H.H. (2008), "Radial spline collocation method for analysis of beams", *Appl. Math. Comput.,* **201**, 184-199.

Yoo, H.H. (1995), "Dynamics of flexible beams undergoing overall motions", *J. Sound Vib.,* **181**(2), 261-278.

Yuh, J. and Young, T. (1990), "Dynamic modeling of an axially moving beam in rotation: simulation and experiment", *J. Dyn. Syst-T. ASME,* **113**, 34-40.

Zhu, W.D. and Ni, J. (2000), "Energetics and stability of translating media with an arbitrarily varying length", *J. Vib. Acoust.,* **122**, 295-304.

Appendix A. Statically condensed discrete equation

Here we use the discrete equation of a boundary value problem to demonstrate the construction of a statically condensed discrete equation for an exact imposition of boundary conditions. Let $\mathbf{B}$ be an $m \times n$ matrix with $m \geq n$, $\mathbf{z}$ be an n -vector, and $\mathbf{q}$ be an m -vector, and express the discrete equation of a boundary value problem as

$$\mathbf{Bz} = \mathbf{q} \tag{60}$$

where

$$\mathbf{B} = \begin{pmatrix} \mathbf{B}_{11} & \mathbf{B}_{12} \\ \mathbf{B}_{21} & \mathbf{B}_{22} \end{pmatrix}, \mathbf{z} = \begin{pmatrix} \hat{\mathbf{z}} \\ \bar{\mathbf{z}} \end{pmatrix}, \mathbf{q} = \begin{pmatrix} \hat{\mathbf{q}} \\ \bar{\mathbf{q}} \end{pmatrix} \tag{61}$$

and $\mathbf{B}_{11}$ is a $(m-k) \times (n-k)$ matrix, $\mathbf{B}_{12}$ is a $(m-k) \times k$ matrix, $\mathbf{B}_{21}$ is a $k \times (n-k)$ matrix, $\mathbf{B}_{22}$ is a $k \times k$ matrix, $\hat{\mathbf{z}}$ is a $(n-k)$ -vector, $\bar{\mathbf{z}}$ is a k -vector, $\hat{\mathbf{q}}$ is a $(m-k)$ -vector, and $\bar{\mathbf{q}}$ is a k -vector. For RBF approximation of a boundary value problem, $\hat{\mathbf{z}}$ and $\bar{\mathbf{z}}$ denote the coefficient vectors of RBF approximation associated with source points located in the domain and boundary, respectively. Here, the first set of equations in (60) are the collocation equations associated with the differential equation, and the second set of equations in (60) are the collocation equations associated with boundary conditions.

We re-write the second set of equation in (60) representing a constraint condition as:

$$\bar{\mathbf{B}}\mathbf{z} = \bar{\mathbf{q}} \tag{62}$$

where

$$\bar{\mathbf{B}} = (\mathbf{B}_{21} \ \mathbf{B}_{22}) \tag{63}$$

Here, $\bar{\mathbf{B}}$ is a $k \times n$ matrix, and $\bar{\mathbf{q}}$ is a k -vector. From Eq. (62), we obtain the following relationship between the independent variable $\hat{\mathbf{z}}$ and dependent variable $\bar{\mathbf{z}}$:

$$\bar{\mathbf{z}} = \mathbf{B}_{22}^{-1}(\bar{\mathbf{q}} - \mathbf{B}_{21}\hat{\mathbf{z}}) \tag{64}$$

Substituting this solution into Eq. (60) yields a reduced system without constrain equations

$$\tilde{\mathbf{B}}\hat{\mathbf{z}} = \tilde{\mathbf{q}} \tag{65}$$

where

$$\tilde{\mathbf{B}} = \mathbf{B}_{11} - \mathbf{B}_{12} \cdot \mathbf{B}_{22}^{-1} \cdot \mathbf{B}_{21} \tag{66}$$

$$\tilde{\mathbf{q}} = \hat{\mathbf{q}} - \mathbf{B}_{12} \cdot \mathbf{B}_{22}^{-1} \cdot \bar{\mathbf{q}} \tag{67}$$

Eq. (65) is called the statically condensed equation of (60) expressed by the independent variable $\hat{\mathbf{z}}$.